Available online at www.sciencedirect.com
SCIENCE DIRECT
Inorganica Chimica Acta 359 (2006) 204–214
Inorganica Chimica Acta
www.elsevier.com/locate/ica

Synthesis, characterisation, supramolecular aggregation and biological activity of phosphine gold(I) complexes with monoanionic thiourea ligands

William Henderson [a,*], Brian K. Nicholson [a], Edward R.T. Tiekink [b,*,1]

[a] *Department of Chemistry, University of Waikato, Private Bag 3105, Hamilton, New Zealand*
[b] *School of Science, Griffith University, Nathan 4111, Qld, Australia*

Received 11 June 2005; accepted 5 July 2005
Available online 23 November 2005

Abstract

A series of phosphine gold(I) complexes containing monoanionic thiourea ligands has been synthesised by reaction of the appropriate precursor chloro complex, Ph_3PAuCl, Cy_3PAuCl, $dppf(AuCl)_2$ [dppf = $Fe(\eta^5\text{-}C_5H_4PPh_2)_2$] or $dppe(AuCl)_2$ (dppe = $Ph_2PCH_2CH_2PPh_2$) with the thiourea and Me_3N base in methanol solution. The complexes have been fully characterised by elemental analysis, NMR spectrometry, electrospray mass spectrometry, and in several cases, by single-crystal X-ray diffraction studies. The crystallographic studies show that the ligands coordinate as a thiolate in each case with systematic variations in geometric parameters being readily ascribed to the influence of the N-bound substituents. In four of the structures, discernable supramolecular aggregation patterns are evident, leading to loosely associated dimers or chain motifs, the latter mediated by either Au···S, N–H···N or C–H···O interactions. Cytotoxicity data, against the P388 leukemia cell line, and anti-microbial data are also reported.

Keywords: Gold; Phosphine complexes; Thiourea complexes; Cytotoxicity; Anti-microbial activity; Supramolecular aggregation

1. Introduction

Phosphine gold(I) thiolate complexes of the type R_3PAuSR' have attracted continued interest in recent years, as a result of their varied and interesting properties. Many compounds of this type are biologically active, indeed the only oral gold–thiolate drug used in the clinic today for treatment of difficult cases of rheumatoid arthritis, *Auranofin*, is a phosphine gold(I) thiolate complex. A range of phosphine gold thiolates has also been shown to have potential as anti-cancer agents [1–5]. The photophysical properties (luminescence) of phosphine gold thiolate complexes also suggest potential applications as sensors, optical materials, etc. [6]. Finally, there is interest in the solid-state structures of such compounds through the formation of Au···Au aurophilic and other interactions [7–11].

We are particularly interested in the chemistry of thiourea derivatives; these can behave as thiolate-type ligands, since a substituted thiourea bearing at least one hydrogen, $R^1R^2NC(=S)NHR^3$ can exist in a tautomeric thiolate form, i.e., $R^1R^2C(SH)=NR^3$. Recently, we have reported studies on complexes of platinum(II) [12], rhodium(III) and ruthenium(II) [13] containing deprotonated and monoanionic thiourea ligands. The most attractive feature of such substituted thioureas is their ease of synthesis, being readily obtained from the amine R^1R^2NH and isothiocyanate R^3NCS, allowing the synthesis of a diverse range of derivatives, with designer properties obtained by varying the substituents R^1, R^2 and R^3. Gold(I) complexes of true

* Corresponding authors. Tel.: +64 7 856 2889; fax: +64 7 838 4219.
E-mail addresses: w.henderson@waikato.ac.nz (W. Henderson), Edward.Tiekink@utsa.edu (E.R.T. Tiekink).
[1] Present address: Department of Chemistry, The University of Texas at San Antonio, Texas 78249-0698, USA.

0020-1693/$ - see front matter © 2005 Elsevier B.V. All rights reserved.
doi:10.1016/j.ica.2005.07.046

trisubstituted thioureas do not appear to have been described to date, although complexes containing deprotonated heterocyclic derivatives that contain the N–C(S)–N grouping, such as 2-thiouracil and 2-mercaptopyrimidine and related compounds, are well known [14–20], and gold(I) phosphine complexes of ligands derived from the closely related carbonimidothiolates (thiocarbamates) PhNHC(S)OR have also been described [21]. In this contribution, we describe the syntheses of a range of phosphine gold(I) complexes of monoanionic thioureas, together with their structural characterisation and biological activity in a P388 murine leukemia screen as well as anti-microbial activity.

2. Results and discussion

2.1. Synthesis and spectroscopic characterisation of phosphine gold(I) thiourea complexes

The reactions of the gold(I) phosphine complexes Ph_3PAuCl, Cy_3PAuCl (Cy = cyclohexyl) and the bisphosphine analogues $dppf(AuCl)_2$ [dppf = $Fe(\eta^5\text{-}C_5H_4PPh_2)_2$] and $dppe(AuCl)_2$ (dppe = $Ph_2PCH_2CH_2PPh_2$) with a range of trisubstituted thioureas $R^1R^2NC(S)NHR^3$ in methanol solution, in the presence of excess trimethylamine base gave a series of phosphine gold(I) complexes containing monoanionic thiourea ligands. The complexes were isolated directly from the reaction mixtures generally in high yields and purities. In a similar manner, the reaction of the commercially available monoanionic thiourea salt Na[MeNHC(S)NCN] with Ph_3PAuCl and $dppe(AuCl)_2$ (without added base) gave the analogous disubstituted complexes **8** and **13** in good yield. The complexes synthesised by this general method are shown in Scheme 1, and contain a range of simple aliphatic, chiral, chromophoric and functional substituents, illustrating the simplicity of this approach in changing the properties of the complex.

The complexes have the expected properties for this class of complex, being stable, and soluble in chlorinated solvents such as dichloromethane, from which they can be recrystallised. They show a single resonance in their $^{31}P\text{–}\{^1H\}$ NMR spectra, at ca. δ 38 for the PPh_3 complexes, and δ 56 for the PCy_3 complexes. The dinuclear complexes also show single ^{31}P resonances. The ^1H NMR spectra were also in accord with the proposed structures. The IR spectra of the complexes show a strong C=N stretch, generally at about 1560 cm^{-1}. The cyanothiourea derivatives **8** and **13** showed a lower C=N stretching frequency, at 1534 cm^{-1} in **8** and 1539 cm^{-1} in **13**, presumably due to conjugation with the cyano functionality, which itself appeared at 2159 and 2151 cm^{-1} in **8** and **13**, respectively.

Electrospray mass spectrometry (ESI-MS) has been successfully used to characterise the new phosphine gold(I) thiourea complexes. However, initial studies carried out in methanol solution using a fairly low cone voltage (20 V) gave, for the triphenylphosphine complexes, the ion $[Au(PPh_3)_2]^+$ (m/z 721) as the base peak in the spectrum, and only very weak $[M+H]^+$ ions. However, the PCy_3 complexes did not give the analogous $[Au(PCy_3)_2]^+$ ion. The high intensity of $[Au(PPh_3)_2]^+$ arises because it is cationic, and therefore even though a solution may only contain a trace of this species, it has high ionisation efficiency relative to a neutral thiourea complex, and hence dominates the spectrum. Significantly improved spectral quality was obtained by using a slightly lower cone voltage (10 V), and by adding a drop of dilute aqueous ammonium acetate solution to the phosphine gold(I) thiourea complex solution. This acts as a mild proton donor, encouraging the formation of $[M+H]^+$ ions. Using this ionisation method, all of the triphenylphosphine and tricyclohexylphosphine complexes gave strong $[M+H]^+$ ions. For some of the PPh_3 complexes, strong $[Au(PPh_3)_2]^+$ ions were still seen, though for most complexes these were quite weak (ca. 10% relative intensity). The majority of the mononuclear phosphine gold complexes also gave the cation $[(Ph_3PAu)_2(\text{monoanionic thiourea})]^+$. This type of species presumably has a structure in which both Ph_3PAu^+ moieties are bound to the thiourea sulfur atom, in comparison with the range of analogous thiolate species of this type which are known [22–27]. The observation of such $[M+AuL]^+$ ions in the spectra of gold(I) thiolate complexes has been observed previously [18,28]. The cyanothiourea complex **8** showed, in addition to the ions described above, a relatively low intensity $[2M+H]^+$ ion (m/z 1164) not observed for the other complexes, presumably due to the greater hydrogen bonding potential in this complex.

The ESI mass spectra of the dinuclear dppe and dppf complexes **11** and **13** are rather different to those of the mononuclear complexes. Thus, for **11** the base peak was the $[M+2H]^{2+}$ ion at m/z 696, where protonation presumably occurs at both thiourea ligands. The dicationic nature was confirmed by the 0.5 m/z separation of adjacent peaks in the isotope pattern, the signature of a dication. A second ion with significant intensity (60%) was the ion $[dppfAu_2\{SC(NPh)N(CH_2CH)_2O\}]^+$ at m/z 1169, formed by loss of a thiourea from the parent $[M+H]^+$ cation (equivalent to loss of a thiourea monoanion from the parent neutral molecule). It is feasible that this ion has the same structure as the species $[(Ph_3PAu)_2SR]^+$ formed in low intensity for the mononuclear complexes. On increasing the cone voltage to 40 V, a new species, identified as $[dppfAu_2\{SC(NPh)N(CH_2CH_2)_2O\}H]^{2+}$ at m/z 585 appeared, formed by loss of a thiourea anion, and protonation. Analogous ions were observed for the dppe complex **12**. In both cases, the $[M+H]^+$ and $[Au(\text{diphosphine})_x]^+$ ($x = 1,2$) ions were not observed.

2.2. Structural studies

Single crystals suitable for X-ray crystallography were obtained for mononuclear complexes **1**, **8** and **10**, and for dinuclear species **11** and **12**. Selected geometric parameters for all structures are compiled in Table 1 and the molecular

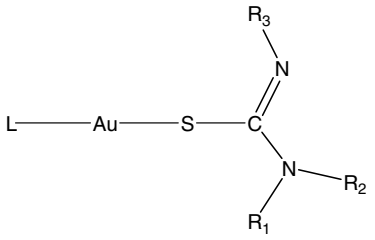

Complex	L	R_1R_2	R_3
1	PPh_3	$(CH_2CH_2)_2O$	Ph
2	PPh_3	$(CH_2CH_2)_2S$	Ph
3	PPh_3	$(CH_2Ph)_2$	Ph
4	PPh_3	Me_2	Ph
5	PPh_3	Me_2	*p*-$C_6H_4NO_2$
6	PPh_3	$(CH_2)_4$	Ph
7	PPh_3	$(CH_2)_5$	Ph
8	PPh_3	HMe	CN
9	PCy_3	Me_2	Ph
10	PCy_3	$(CH_2CH_2)_2O$	Ph

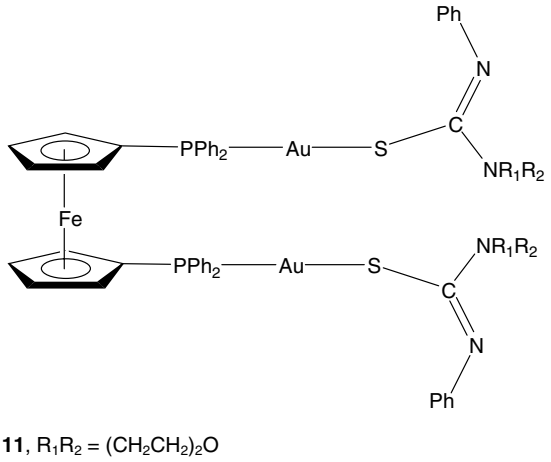

11, $R_1R_2 = (CH_2CH_2)_2O$

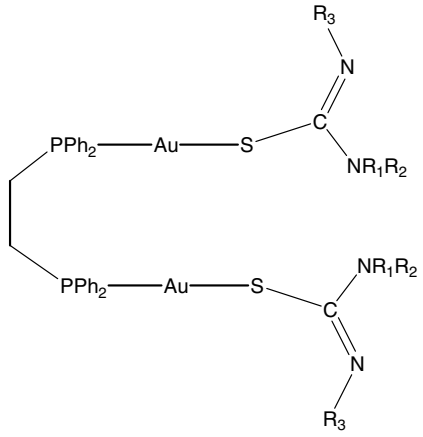

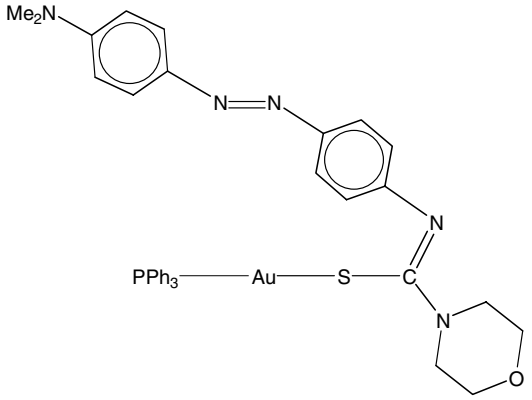

14

Complex	R_1R_2	R_3
12	$(CH_2CH_2)_2O$	Ph
13	HMe	CN

Scheme 1. Phosphinegold(I) thiourea complexes described in this work.

structures are illustrated in Figs. 1–5. The molecular structure of **1** features a linearly coordinated gold centre defined by S and P donor atoms; this coordination motif is repeated in all of the remaining structures to be described herein. An examination of the bond distances associated with the deprotonated thiourea ligand reveals a number of interesting observations. First, and foremost, these indicate that this ligand is coordinating as a thiolate ligand. There is some evidence for some delocalization of π-electron density over the thiolate ligand but this is restricted as there are significant twists in the bonds describing the Au–thiolate residue, as indicated by the values of the relevant torsion angles collected in Table 1, and also within the thiolate ligand itself. Thus, while the formally S–C1=N2–C11 residue is essentially planar, this is not extended to the N1-containing portion of the thiolate. In keeping with this, the C1=N2 bond distance is significantly shorter than the C1–N1 bond distance consistent with significant localization of π-electron density in the C1=N2 bond. In terms of angles, the S1–C1–N2 angle is at least 10° greater than

Table 1
Selected bond distances (Å) and angles (°) for **1**, **8**, **10**, **11**[a] and **12** · CH_2Cl_2[a]

Parameter	1	8	10	11	12 · CH_2Cl_2
Au–S1	2.3115(7)	2.3075(15)	2.3044(4)	2.3112(12), 2.3009(12)	2.3066(14), 2.2782(15)
Au–P1	2.2628(6)	2.2674(15)	2.2701(4)	2.2546(11), 2.2561(11)	2.2638(13), 2.2530(13)
S1–C1	1.772(3)	1.746(7)	1.7765(18)	1.776(4), 1.782(4)	1.772(5), 1.768(7)
C1–N1	1.383(3)	1.336(8)	1.384(2)	1.361(5), 1.374(5)	1.386(7), 1.365(8)
C1–N2	1.287(3)	1.331(9)	1.282(2)	1.282(5), 1.270(5)	1.276(7), 1.272(9)
S1–Au–P1	169.29(2)	172.83(6)	167.340(16)	170.43(4), 169.32(4)	166.67(5), 169.91(5)
Au–S1–C1	109.92(9)	108.7(2)	110.21(6)	107.39(16), 106.85(15)	108.82(18), 108.9(2)
S1–C1–N1	114.21(18)	114.4(5)	113.41(13)	114.9(3), 113.7(3)	114.1(4), 112.8(5)
S1–C1–N2	128.4(2)	128.1(5)	128.53(14)	127.3(4), 127.6(4)	127.7(4), 128.3(5)
N1–C1–N2	117.3(2)	117.4(6)	117.95(16)	117.8(4), 118.5(4)	118.2(5), 119.0(6)
Au/S1/C1/N1	161.00(17)	−146.1(4)	−151.94(11)	152.4(3), 143.9(3)	148.3(4), 175.7(5)
Au/S1/C1/N2	−21.8(3)	36.5(6)	31.99(19)	−26.0(4), −40.6(5)	−28.2(6), −2.8(8)
S1/C1/N1/C2	−40.3(3)	−179.9(5)	38.3(2)	−1.2(8), −31.9(6)	26.2(7), −7.9(12)
S1/C1/N2/C11	−12.7(4)	−4.0(9)	9.7(3)	−9.3(7), −5.9(7)	−5.3(9), −9.5(12)

[a] Two independent molecules comprise the asymmetric unit. Parameters for the second independent molecule follow those listed for the first.

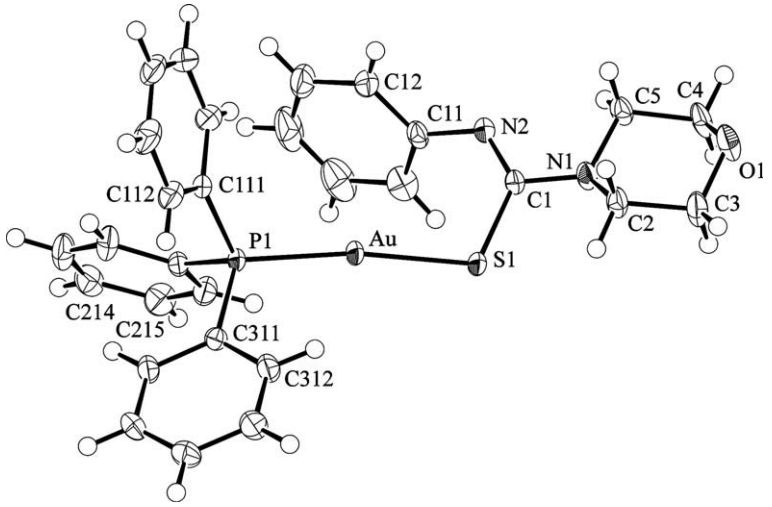

Fig. 1. Molecular structure of $Ph_3PAuSC(=NPh)N(CH_2CH_2)_2O$ (**1**) showing the atomic numbering scheme.

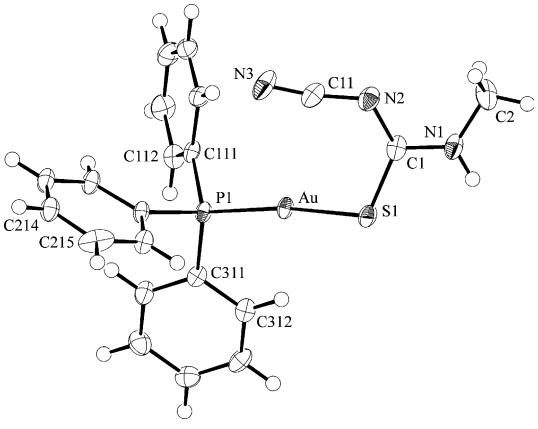

Fig. 2. Molecular structure of $Ph_3PAuSC(=NCN)N(H)Me$ (**8**) showing the atomic numbering scheme.

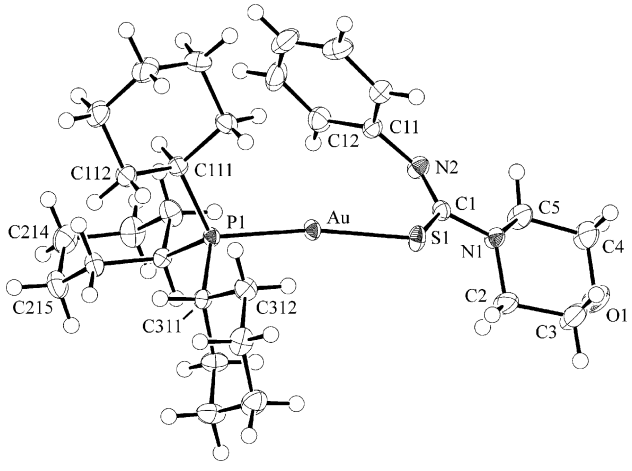

Fig. 3. Molecular structure of $Cy_3PAuSC(=NPh)N(CH_2CH_2)_2O$ (**10**) showing the atomic numbering scheme.

the other angles subtended at the C1 atom, with the narrowest of these being the S1–C1–N1 angle, i.e., opposite the formal N=C double bond. As can be seen from Fig. 1, the thiolate ligand is orientated so as to place the aromatic ring in proximity to the Au atom. The distance between the Au atom and the centroid of the aromatic ring

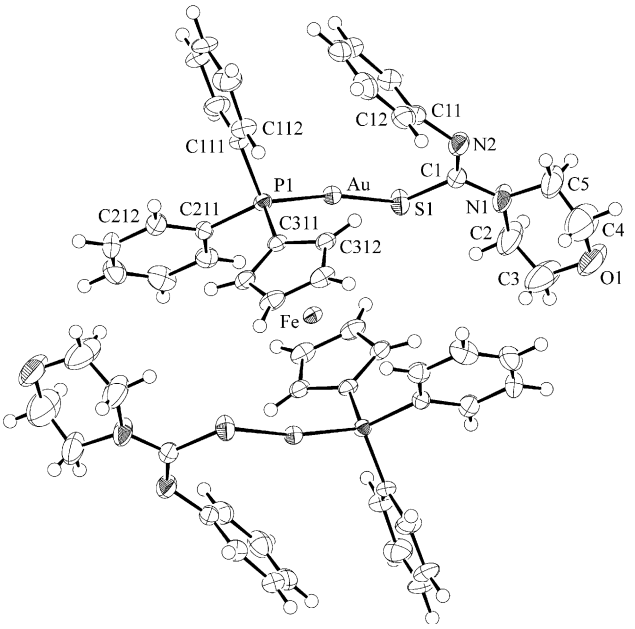

Fig. 4. Molecular structure of dppf[AuSC(=NPh)N(CH_2CH_2)$_2$O]$_2$ (**11**) showing the atomic numbering scheme.

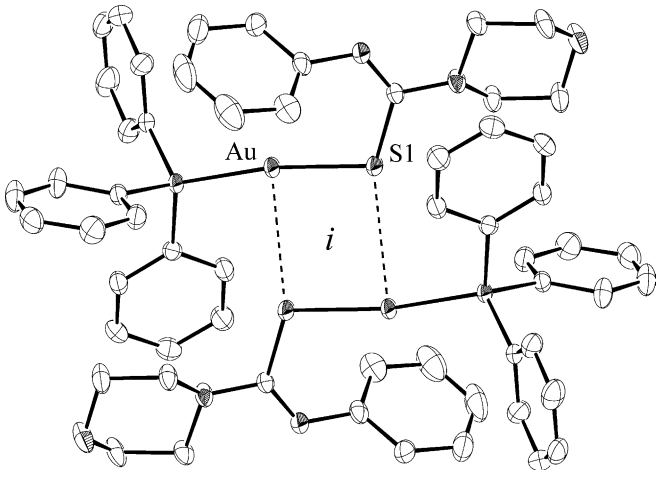

Fig. 6. Supramolecular aggregation leading to dimer formation via Au···S interactions in the structure of $Ph_3PAuSC(=NPh)N(CH_2CH_2)_2O$ (**1**); H atoms have been omitted for clarity.

is 3.4449(18) Å. However, it is noted that the Au···C separations are far from symmetric as they span a range 3.160(3)–4.204(5) Å, possibly reflecting the constraints of the S1–C1–N2 angle. The molecular structure of **8** is in essential agreement with that just described. It is noteworthy that the disparity in the C–N1, N2 distances apparent in **1** no longer seem to pertain in **8**. Also, noteworthy is the observation that the C–S distance is significantly shorter in **8** compared to **1**. These variations coupled with the planarity within the thiolate ligand, Table 1, suggests significantly more delocalization over the central chromophore of the thiolate ligand, a feature that can be ascribed to the electron-withdrawing nature of the cyanide group. Again, the N2-bound organic residue is orientated so as to be close to the Au atom, consistent with a Au···π interaction; Au···C11 is 3.166(6) Å and Au···N3 is 3.331(6) Å. The geometric features of the molecular structure of **10**, having the identical N1- and N2-bound groups as in **1**, are essentially in agreement with those of **1**. Here, the Au···ring centroid separation involving the C11–C16 ring is 3.58 Å, suggesting a weaker interaction compared to that in **1**, an observation ascribed to the greater steric bulk of the cyclohexylphosphine ligand. Thus, whereas the longest Au···C separation involving the aromatic ring in **1** was 4.204(5) Å, for Au···C14, and the longest comparable separation in **10** was 4.333(2) Å. Similar coordination geometries are found in the dinuclear gold compounds **11** and **12**.

Two independent "half" molecules comprise the asymmetric unit in **11**. Each of the molecules is situated on a crystallographic centre of inversion, i.e., the Fe atom is situated on a site of symmetry, $\bar{1}$. Only one molecule is illustrated in Fig. 4 as the second independent molecule is essentially identical, at least in terms of its molecular geometry. The major difference in the geometric parameters describing the two molecules is found in the planarity of the thiolate ligands, i.e., the thiolate ligand for molecule a is essentially planar compared to a twisted conformation in molecule b. The distance between the Au atom and the

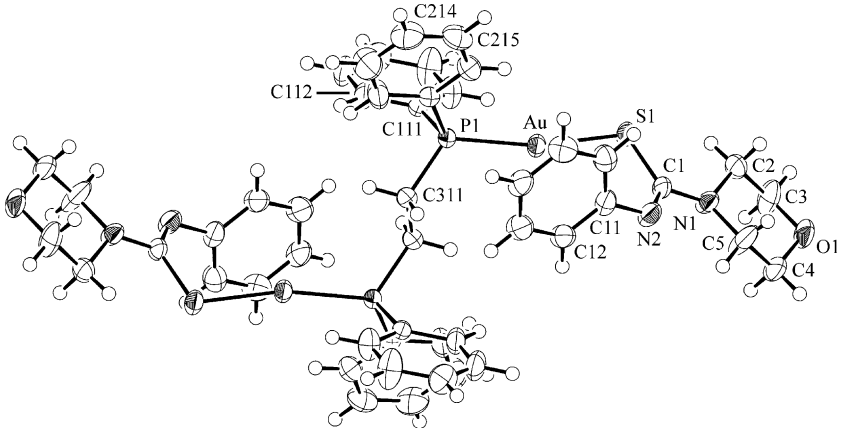

Fig. 5. Molecular structure of dppe[AuSC(=NPh)N(CH_2CH_2)$_2$O]$_2$ (**12**) showing the atomic numbering scheme.

C11–C16 ring centroid for molecule a is 3.3482(18) Å; this is significantly longer at 3.504(2) Å for the molecule b. The conformation of each of the independent molecules, as a result of the crystallographic symmetry, is *trans*. Two independent molecules are also found in the crystal structure of **12**. In this case, two molecules, each disposed about a crystallographic centre of inversion as well as a dichloromethane molecule of solvation comprise the asymmetric unit so that the ratio of dinuclear complex to solvent is 1:1; only one independent molecule is shown in Fig. 5. In terms of molecular geometry, the major conformational difference between the independent molecules in **12**, as for **11**, is found in the planarity of the thiolate ligands, see Table 1. The distances between the Au atoms and the respective ring centroids of the C11–C16 rings are 3.281(3) and 3.286(5) Å, respectively. The bond distances defining the thiolate molecules in dinuclear **11** and **12** resemble those found in mononuclear **1** and **10**, i.e., indicating localization of π-electron density in the S–C–N2–C portion of the ligand.

Recognisable supramolecular association patterns are discernable in several of the crystal structures, just described. In the crystal structure of **1**, molecules associate via the formation of $[Au\cdots S]_2$ rectangles so that $Au\cdots S1^{i}$ is 3.4211(7) Å for symmetry operation i: $-x, -y, -z$; this association is represented in Fig. 6. In **8**, rather than the formation of the expected $[S–C–N–H]_2$ synthon, molecules associate via N–H···NC interactions so as to form a chain motif, as illustrated in Fig. 7. The parameters associated with this interaction are $N1–H\cdots N3^{ii}$ of 2.22 Å, $N1\cdots N3^{ii}$ of 2.995(8) Å, and an angle subtended at H of 147°, for symmetry operation ii: $-1/2 - x, -1/2 + y, 1/2 - z$. In **10**, the molecules pack via hydrophobic interactions, with close association, as found in **1**, most likely precluded owing to the steric bulk of the cyclohexylphosphine ligands. In **11**, the independent molecules are connected via C–H···O interactions as to form a chain arrangement as shown in Fig. 8. Thus, the H12a atoms of molecule a are connected to O1b atoms of molecule b with

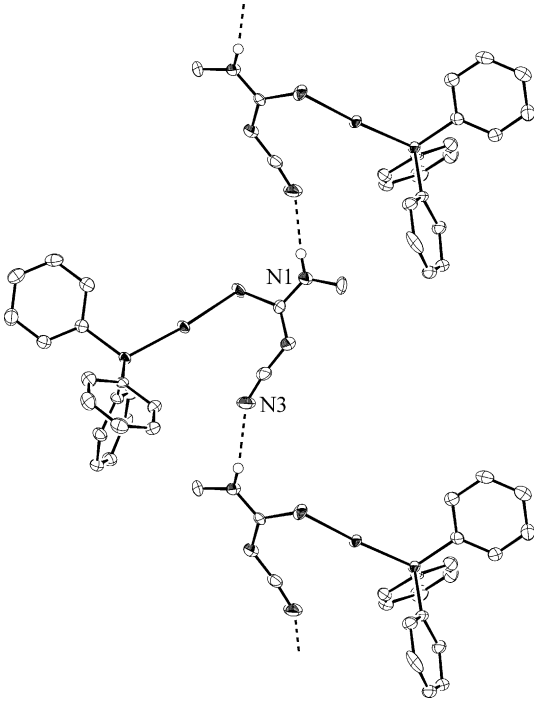

Fig. 7. Supramolecular aggregation leading to a chain motif mediated by N–H···N interactions in the structure of $Ph_3PAuSC(=NCN)N(H)Me$ (**8**); non-participating H atoms have been omitted for clarity.

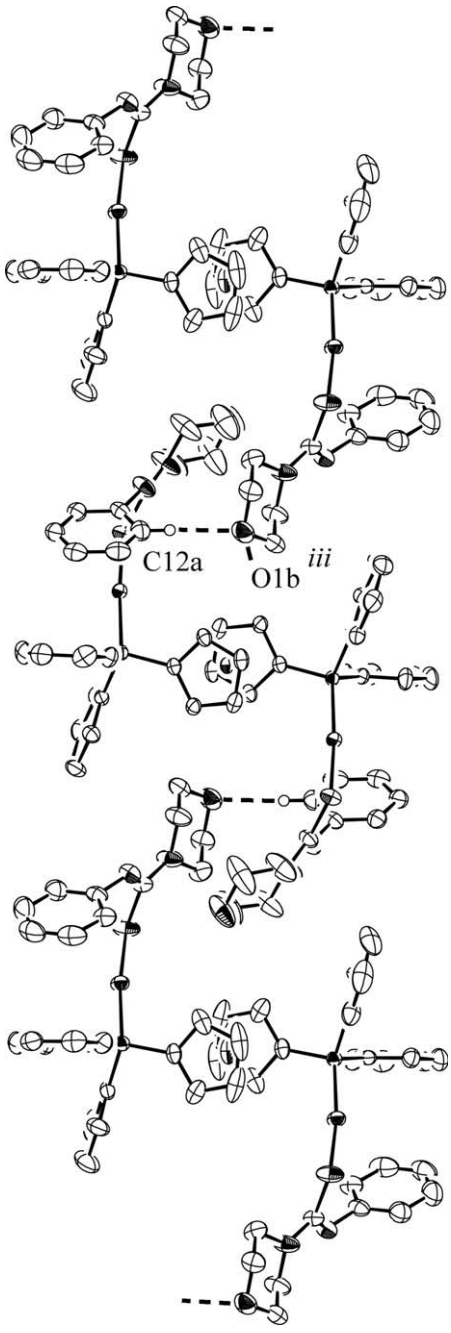

Fig. 8. Supramolecular aggregation leading to a chain motif mediated by C–H···O interactions in the structure of $dppf[AuSC(=NPh)N(CH_2CH_2)_2O]_2$ (**11**); non-participating H atoms have been omitted for clarity.

C12a–H···O1b^{iii} of 2.45 Å, C12a···O1b^{iii} of 3.370(5) Å and an angle of 165° subtended at H for symmetry operation iii: $-x, -1-y, -z$. Finally, in the crystal structure of **12**, two distinct supramolecular motifs are observed. A chain motif, mediated via weak $[Au\cdots S]_2$ interactions, akin to those observed in **1** are found. The magnitude of the individual Au···S interactions is somewhat longer than that observed in **1**, i.e., Au···S1^{iv} is 3.8771(16) Å for symmetry operation iv: $-x, -1-y, 1-z$, nevertheless, a discernable supramolecular motif, i.e., a linear chain, is apparent as represented in Fig. 9(a). Similar supramolecular aggregation is not observed for the second independent molecule in **12** as the solvent CH_2Cl_2 molecules are associated with the S atoms, thereby blocking these off for analogous $[Au\cdots S]_2$ association as found between molecules of a. Thus, the C100–H···S1b^{v} separation is 2.82 Å, C100–H···S1b^{v} is 3.725(19) Å and the angle at H is 153° for symmetry operation v: $1-x, 1-y, 1-z$. Despite this avenue for aggregation being precluded, i.e., Au···S interactions, a chain motif is still apparent, akin to that observed in **11** and as shown in Fig. 9(b). Thus, molecules of b form a chain via the following interactions: C512–H···O1b^{vi} is 2.58 Å, C512 ···O1b^{vi} is 3.451(10) Å with an angle of 155° subtended at H for symmetry operation vi: $-1-x, 1-y, -z$.

2.3. Biological activity of phosphinegold(I) thiourea complexes

Because many gold(I) thiolate complexes have been found to show potential and actual anti-cancer activity [1,2], a selection of the phosphine gold(I) thiourea complexes described in this paper has been screened for activity against P388 murine leukemia cells. The antimicrobial activity of the same complexes was also assayed, against three bacteria and three fungi. Data are summarised in Table 2. The complexes generally have moderate to low cytotoxicity, though the compounds with greatest activity appear to be those with small, hydrophobic alkyl substituents in the R_1 and R_2 positions, Scheme 1. All complexes displayed very low or no antimicrobial activity, the most activity being obtained for the tricyclohexylphosphine complex **9**.

3. Experimental

3.1. General

^{1}H, ^{13}C–{^{1}H} and ^{31}P–{^{1}H} NMR spectra were recorded on a Bruker AC300P spectrometer in $CDCl_3$ unless otherwise stated. Elemental analyses were obtained

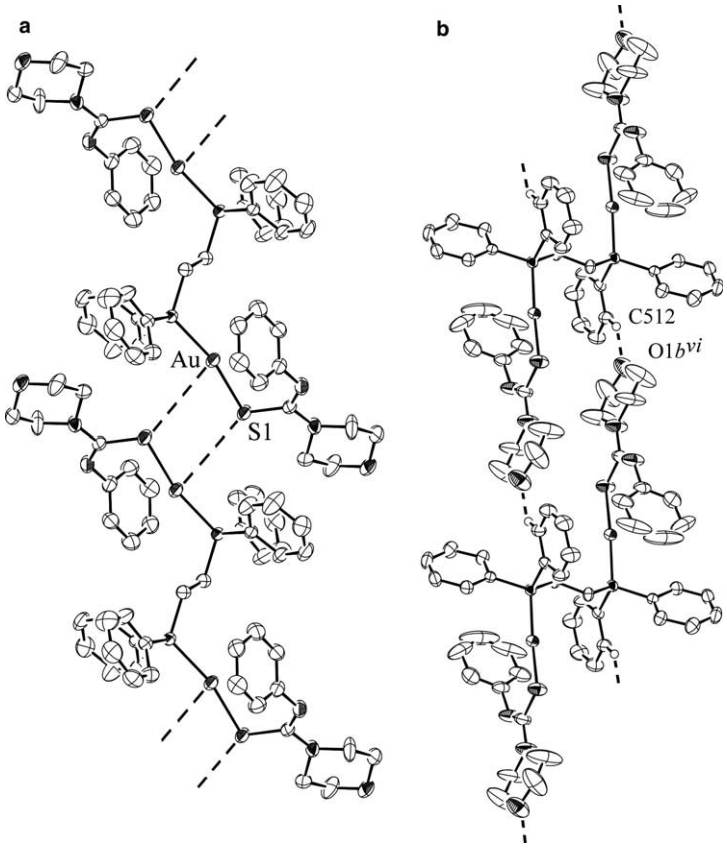

Fig. 9. Supramolecular aggregation leading to chain motifs in the structure of dppe[AuSC(=NPh)N(CH$_2$CH$_2$)$_2$O]$_2$ (**12**), (a) via Au···S interactions between molecules of a, and (b) via C–H···O interactions between molecules of b; non-participating H atoms and solvent CH_2Cl_2 molecules have been omitted for clarity.

Table 2
In vitro cytotoxicity and antimicrobial/antifungal activity data for the phosphine gold(I) thiourea complexes

Complex	IC_{50}(μM)[a]	Antimicrobial activity[b,c]					
		Ec	Bs	Pa	Ca	Tm	Cr
1	4.2		2			1	1
2	1.5		2			1	
3	5.8		1				
4	1.6		3			1	3
6	<1.5		2			1	2
7	<1.4		2			1	2
9	1.8	1	3		3	3	4
10	6.0		1			1	
11	5.3		1				
12	9.9		3		2		
13	31.1		1				
14	42.0		1				

[a] The concentration of sample in μM required to reduce the cell growth of the P388 leukemia cell line (ATCC CCL 46) by 50%.

[b] Inhibition zone as excess radius (mm) from a 6 mm (diameter) disc containing 2 μg of sample. No entry indicates lack of activity.

[c] Ec, *Escherichia coli*; Bs, *Bacillus subtilis*; Pa, *Pseudomonas aeruginosa*; Ca, *Candida albicans*; Tm, *Trichophyton mentagrophytes*; and Cr, *Cladosporium resinae*.

by the Campbell Microanalytical Laboratory at the University of Otago, Dunedin, New Zealand.

ESI mass spectra were recorded on a VG Platform II instrument in positive-ion mode, using methanol as the mobile phase. Several drops of a dilute ammonium acetate solution (concentration ca. 1 g L^{-1}) were added to the analyte solution to aid in protonation. Spectra were recorded at a low cone voltage (10 V) to minimise fragmentation. Infrared spectra were recorded as KBr disks on a Bio-Rad FTS40 spectrophotometer. Melting points were determined on a Reichert-Jung hotstage apparatus and are uncorrected.

All reactions were carried out in laboratory reagent grade methanol without further purification. Dichloromethane and diethyl ether were purified by distillation from calcium hydride and sodium-benzophenone ketyl, respectively.

The complexes Ph_3PAuCl [29], Cy_3PAuCl [30], dppf$(AuCl)_2$ [31], and dppe$(AuCl)_2$ [32] were prepared by the literature methods. The thioureas PhNHC(S)N$(CH_2CH_2)_2O$, PhNHC(S)N$(CH_2Ph)_2$, PhNHC(S)NMe_2, and $Me_2NC_6H_4N{=}NC_6H_4NHC(S)N(CH_2CH_2)_2O$ were prepared from the appropriate isothiocyanate and amine, as described previously [12]. The sodium salt Na[MeNHC(S)NCN] (Aldrich) and aqueous trimethylamine (BDH, 25–30% w/v) were used as supplied. PhNHC(S)N$(CH_2CH_2)_2S$, PhNHC(S)N$(CH_2)_4$, PhNHC(S)N$(CH_2)_5$, and *p*-$O_2NC_6H_4NHC(S)NMe_2$ were prepared by reaction of an ether solution of PhNCS with, respectively, thiomorpholine (Aldrich), pyrrolidine (BDH), piperidine (BDH) or *p*-nitroaniline (BDH). Melting points: PhNHC(S)N$(CH_2CH_2)_2S$ 159–162 °C, PhNHC(S)N$(CH_2)_4$ 119–120 °C, PhNHC(S)N$(CH_2)_5$ 97–98 °C.

3.2. Synthesis of phosphinegold(I) monoanionic thiourea complexes – general method

The precursor phosphinegold chloride complex [Ph_3PAuCl, Cy_3PAuCl, dppe$(AuCl)_2$ or dppf$(AuCl)_2$] and the thiourea (1 mole equivalent per gold) were suspended in methanol (20–25 mL), at which time the starting materials often dissolved to give a clear solution. The mixture was warmed to ca. 60 °C, aqueous trimethylamine (2–3 mL, excess) added, and the mixture heated to reflux for a few minutes. Water (10–30 mL) was then added, the mixture cooled to room temperature, and the solid product filtered off, washed with water (2 × 10mL) and dried under vacuum.

The following complexes were synthesised by this method.

3.2.1. $Ph_3PAuSC(=NPh)N(CH_2CH_2)_2O$ (**1**)

Ph_3PAuCl (400 mg, 0.809 mmol) with PhNHC(S)N$(CH_2CH_2)_2O$ (180 mg, 0.811 mmol) gave white microcrystals of **1** (480 mg, 87%). M.p. 168–178 °C. *Anal.* Calc. for $C_{29}H_{28}N_2AuOPS$: C, 51.2; H, 4.15; N, 4.1. Found: C, 51.3; H, 4.1; N, 4.1%. $^{31}P-\{^1H\}$ NMR, δ 38.4 (s). ^1H NMR, δ 7.54–6.40 (m, Ph), 3.87 (m, CH_2O), 3.37 (m, CH_2N). ESI-MS, *m*/*z* 681 $[M+H]^+$ (100%), 721 $[Au(PPh_3)_2]^+$ (10%), 1139 $[(Ph_3PAu)_2SC(NPh)N(CH_2CH_2)_2O]^+$ (5%). IR ν_{max} 1556 cm^{-1} (s).

3.2.2. $Ph_3PAuSC(=NPh)N(CH_2CH_2)_2S$ (**2**)

Ph_3PAuCl (300 mg, 0.607 mmol) with PhNHC(S)N$(CH_2CH_2)_2S$ (145 mg, 0.609 mmol) gave a white powder of **2** (360 mg, 85%). M.p. 148–152 °C. *Anal.* Calc. for $C_{29}H_{28}N_2AuPS_2$: C, 50.0; H, 4.05; N, 4.0. Found: C, 50.0; H, 3.9; N, 4.01%. $^{31}P-\{^1H\}$ NMR, δ 38.4 (s). ^1H NMR, δ 7.55–6.40 (m, Ph), 4.24 (m, CH_2), 2.72 (m, CH_2). ESI-MS, *m*/*z* 697 $[M+H]^+$ (100%), 721 $[Au(PPh_3)_2]^+$ (15%), 1155 $[(Ph_3PAu)_2SC(NPh)N(CH_2CH_2)_2S]^+$ (5%). IR ν_{max} 1560 cm^{-1} (s).

3.2.3. $Ph_3PAuSC(=NPh)N(CH_2Ph)_2$ (**3**)

Ph_3PAuCl (300 mg, 0.607 mmol) with PhNHC(S)N$(CH_2Ph)_2$ (201 mg, 0.605 mmol) gave white microcrystals of **3** (444 mg, 93%). M.p. 54–58 °C. *Anal.* Calc. for $C_{39}H_{34}N_2AuPS$: C, 59.2; H, 4.3; N, 3.5. Found: C, 59.3; H, 4.2; N, 3.7%. $^{31}P-\{^1H\}$ NMR, δ 38.2 (s). ^1H NMR, δ 7.53–6.43 (m, Ph), 4.99 (s, CH_2). ESI-MS, *m*/*z* 721 $[Au(PPh_3)_2]^+$ (10%), 791 $[M+H]^+$ (100%), 1249 $[(Ph_3PAu)_2SC(NPh)N(CH_2Ph)_2]^+$ (2%). IR ν_{max} 1560 cm^{-1} (s).

3.2.4. $Ph_3PAuSC(=NPh)NMe_2$ (**4**)

Ph_3PAuCl (200 mg, 0.404 mmol) with PhNHC(S)NMe_2 (73 mg, 0.406 mmol) gave white microcrystals of **4** (220 mg, 85%). M.p. 76–79 °C. *Anal.* Calc. for $C_{27}H_{26}N_2AuPS$: C, 50.8; H, 4.1; N, 4.4. Found: C, 49.9; H, 4.0; N, 4.3%. $^{31}P-\{^1H\}$ NMR, δ 38.4 (s). ^1H NMR, δ 7.51–6.38 (m, Ph), 3.29 (s, Me). ESI-MS, *m*/*z* 639 $[M+H]^+$ (100%), 721

$[Au(PPh_3)_2]^+$ (5%), 1097 $[(Ph_3PAu)_2SC(NPh)NMe_2]^+$ (5%). IR ν_{max} 1560 cm^{-1} (s).

3.2.5. $Ph_3PAuSC(=NC_6H_4NO_2\text{-}p)NMe_2$ (5)

Ph_3PAuCl (200 mg, 0.404 mmol) with $p\text{-}O_2NC_6H_4NHC(S)NMe_2$ (91 mg, 0.404 mmol) gave bright-yellow microcrystals of **5** (230 mg, 83%). M.p. 144–146 °C. *Anal.* Calc. for $C_{27}H_{25}N_3AuO_2PS$: C, 47.4; H, 3.7; N, 6.15. Found: C, 47.5; H, 3.6; N, 6.2%. $^{31}P–\{^1H\}$ NMR, δ 38.1 (s). ^1H NMR, δ 7.64–6.70 (m, Ph), 3.31 (s, NMe_2). ESI-MS, *m/z* 684 $[M+H]^+$ (100%), 721 $[Au(PPh_3)_2]^+$ (18%), 1142 $[(Ph_3PAu)_2SC(NC_6H_4NO_2\text{-}p)NMe_2]^+$ (5%). IR ν_{max} 1560 cm^{-1} (s).

3.2.6. $Ph_3PAuSC(=NPh)N(CH_2)_4$ (6)

Ph_3PAuCl (150 mg, 0.303 mmol) with $PhNHC(S)N(CH_2)_4$ (63 mg, 0.306 mmol) gave white microcrystals of **6** (190 mg, 95%). M.p. 168–172 °C. *Anal.* Calc. for $C_{29}H_{28}N_2AuPS$: C, 52.4; H, 4.25; N, 4.2. Found: C, 52.4 H, 4.3; N, 4.1%. $^{31}P–\{^1H\}$ NMR, δ 38.5 (s). ^1H NMR, δ 7.51–6.33 (m, Ph), 3.76 [t, NCH_2, ^3J(HH) 6.7], 1.94 (m, CH_2). ESI-MS, *m/z* 665 $[M+H]^+$ (100%), 721 $[Au(PPh_3)_2]^+$ (4%), 1123 $[(Ph_3PAu)_2SC(NPh)N(CH_2)_4]^+$ (4%). IR ν_{max} 1540 cm^{-1} (s).

3.2.7. $Ph_3PAuSC(=NPh)N(CH_2)_5$ (7)

Ph_3PAuCl (150 mg, 0.303 mmol) with $PhNHC(S)N(CH_2)_5$ (67 mg, 0.305 mmol) gave a white powder of **7** (183 mg, 89%). M.p. 132–135 °C. *Anal.* Calc. for $C_{30}H_{30}N_2AuPS$: C, 53.1; H, 4.5; N, 4.1. Found: C, 53.1; H, 4.4; N, 4.1%. $^{31}P–\{^1H\}$ NMR, δ 38.4 (s). ^1H NMR, δ 7.52–6.41 (m, Ph), 3.86 (s, br), 1.65 (s, br). ESI-MS, *m/z* 679 $[M+H]^+$ (100%), 721 $[Au(PPh_3)_2]^+$ (8%), 1137 $[(Ph_3PAu)_2SC(NPh)N(CH_2)_5]^+$ (5%). IR ν_{max} 1558 cm^{-1} (s).

3.2.8. $Cy_3PAuSC(=NPh)NMe_2$ (9)

Cy_3PAuCl (250 mg, 0.488 mmol) with $PhNHC(S)NMe_2$ (100 mg, 0.556 mmol) gave a white powder of **9** (266 mg, 83%). M.p. 131–133 °C. *Anal.* Calc. for $C_{27}H_{44}N_2AuPS$: C, 49.4; H, 6.75; N, 4.3. Found: C, 49.1; H, 6.9; N, 4.2%. $^{31}P–\{^1H\}$ NMR, δ 55.9 (s). ^1H NMR, δ 7.28–6.81 (m, Ph), 3.28 (s, NMe_2), 1.81–1.26 (m, Cy). ESI-MS, *m/z* 657 $[M+H]^+$ (100%), 1133 $[(Cy_3PAu)_2SC(NPh)NMe_2]^+$ (3%). IR ν_{max} 1558 cm^{-1} (s).

3.2.9. $Cy_3PAuSC(=NPh)N(CH_2CH_2)_2O$ (10)

Cy_3PAuCl (200 mg, 0.390 mmol) with $PhNHC(S)N(CH_2CH_2)_2O$ (87 mg, 0.392 mmol) gave a white powder of **10** (270 mg, 99%). M.p. 214–218 °C. *Anal.* Calc. for $C_{29}H_{46}N_2AuOPS$: C, 49.85; H, 6.6; N, 4.0. Found: C, 49.6; H, 6.8; N, 4.2%. $^{31}P–\{^1H\}$ NMR, δ 56.4 (s). ^1H NMR, δ 7.28–6.81 (m, Ph), 3.87 (m, CH_2O), 3.76 (m, CH_2N), 1.84–1.27 (m, Cy). ESI-MS, *m/z* 699 $[M+H]^+$ (100%), 1175 $[(Cy_3PAu)_2SC(NPh)N(CH_2CH_2)_2O]^+$ (3%). IR ν_{max} 1560 cm^{-1} (s).

3.2.10. $dppf[AuSC(=NPh)N(CH_2CH_2)_2O]_2$ (11)

The complex $dppf(AuCl)_2$ (200 mg, 0.196 mmol) with $PhNHC(S)N(CH_2CH_2)_2O$ (87 mg, 0.392 mmol) gave an orange powder of **11** (220 mg, 81%). M.p. 197–202 °C. *Anal.* Calc. for $C_{56}H_{54}N_4Au_2FeO_2P_2S_2$: C, 48.35; H, 3.9; N, 4.0. Found: C, 48.3; H, 3.8; N, 4.0%. $^{31}P–\{^1H\}$ NMR, δ 32.7 (s). ^1H NMR, δ 7.50–6.42 (m, Ph), 4.55 (s, FeC_5H_4), 4.04 (s, FeC_5H_4), 3.87 (s, CH_2O), 3.77 (s, CH_2N). ESI-MS, *m/z* 696 $[M+2H]^{2+}$ (100%), 1169 $[dppfAu_2\{SC(NPh)N(CH_2CH_2)_2O\}]^+$ (60%). IR ν_{max} 1567 cm^{-1} (s).

3.2.11. $dppe[AuSC(=NPh)N(CH_2CH_2)_2O]_2$ (12)

The complex $dppe(AuCl)_2$ (200 mg, 0.232 mmol) with $PhNHC(S)N(CH_2CH_2)_2O$ (103 mg, 0.464 mmol) gave a white powder of **12** (230 mg, 80%). M.p. 160–166 °C. *Anal.* Calc. for $C_{48}H_{50}N_4Au_2O_2P_2S_2$: C, 46.7; H, 4.1; N, 4.5. Found: C, 46.2; H, 3.9; N, 4.4%. $^{31}P–\{^1H\}$ NMR, δ 36.3 (s). ^1H NMR, δ 7.57–6.36 (m, Ph), 3.86 (m, CH_2O), 3.78 (m, CH_2N), 2.26 (s, CH_2). ESI-MS, *m/z* 618 $[M+2H]^{2+}$ (100%), 1013 $[dppeAu_2\{SC(NPh)N(CH_2CH_2)_2O\}]^+$ (60%). IR ν_{max} 1559 cm^{-1} (s).

3.2.12. $Ph_3PAuSC(=NC_6H_4N{=}NC_6H_4NMe_2)N(CH_2CH_2)_2O$ (14)

Ph_3PAuCl (150 mg, 0.303 mmol) with $Me_2NC_6H_4N{=}NC_6H_4NHC(S)N(CH_2CH_2)_2O$ (114 mg, 0.312 mmol) gave bright-orange microcrystals of **14** (230 mg, 92%). M.p. 196–200 °C. *Anal.* Calc. for $C_{37}H_{37}N_5AuOPS$: C, 53.7; H, 4.5; N, 8.5. Found: C, 53.8; H, 4.6; N, 8.5%. $^{31}P–\{^1H\}$ NMR, δ 38.1 (s). ^1H NMR, δ 7.72–6.75 (m, Ph), 3.91 (m, CH_2O), 3.79 (m, CH_2N), 3.09 (s, NMe_2). ESI-MS, *m/z* 721 $[Au(PPh_3)_2]^+$ (65%), 828 $[M+H]^+$ (100%). IR ν_{max} 1540 cm^{-1} (s).

3.3. Synthesis of $Ph_3PAuSC(=NCN)NHMe$ (8)

A suspension of Ph_3PAuCl (200 mg, 0.404 mmol) and Na[MeNHC(S)NCN] (60 mg, 0.438 mmol) in methanol (15 mL) was stirred at room temperature for 48 h. To the white suspension was added water (20 mL), and the white solid filtered off, washed with water (10 mL) and petroleum spirits (10 mL) and dried under vacuum to give **8** (200 mg, 87%). M.p. 158–160 °C. *Anal.* Calc. for $C_{21}H_{19}N_3AuPS$: C, 44.0; H, 3.3; N, 7.3. Found: C, 44.0; H, 3.2; N, 7.4%. $^{31}P–\{^1H\}$ NMR, δ 37.3 (s). ^1H NMR, δ 7.65–7.45 (m, Ph), 5.97 (s, br, NH), 2.91 [d, Me, J(HH) 4.7]. ESI-MS, *m/z* 574 $[M+H]^+$ (100%), 721 $[Au(PPh_3)_2]^+$ (90%), 1032 $[(Ph_3PAu)_2SC(NCN)NHMe]^+$ (5%), 1164 $[2M+H]^+$ (10%). IR ν_{max} 2159 (s) and 1534 (s) cm^{-1}.

3.4. Synthesis of $dppe[AuSC(=NCN)NHMe]_2$ (13)

A suspension of $dppe(AuCl)_2$ (200 mg, 0.231 mmol) and Na[MeNHC(S)NCN] (70 mg, 0.511 mmol) in methanol (25 mL) was stirred at room temperature, rapidly giving a clear colourless solution, which then deposited a white

Table 3
Crystallographic data and refinement details for **1**, **8**, **10**, **11** and **12** · CH_2Cl_2

Complex	**1**	**8**	**10**	**11**	**12** · CH_2Cl_2
Formula	$C_{29}H_{28}AuN_2OPS$	$C_{21}H_{19}AuN_3PS$	$C_{29}H_{46}AuN_2OPS$	$C_{56}H_{54}Au_2FeN_4O_2P_2S_2$	$C_{48}H_{50}Au_2N_4O_2P_2S_2 \cdot CH_2Cl_2$
Molecular weight	680.53	573.39	698.67	1390.88	1319.84
T/K	223	168	223	223	223
Crystal system	triclinic	monoclinic	triclinic	monoclinic	triclinic
Space group	$P\bar{1}$	$P2_1/n$	$P\bar{1}$	$P2_1/n$	$P\bar{1}$
a (Å)	8.8802(5)	8.155(2)	10.2467(5)	22.7135(13)	11.6971(7)
b (Å)	12.5815(7)	14.290(3)	11.0923(6)	9.7423(5)	11.9933(8)
c (Å)	13.1321(7)	17.431(4)	13.5082(7)	24.2348(13)	19.0573(12)
α (°)	111.443(1)	90	80.747(1)	90	81.529(1)
β (°)	107.180(1)	92.865(3)	71.612(1)	110.312(1)	72.568(1)
γ (°)	92.425(1)	90	84.415(1)	90	74.016(2)
V (Å^3)	1285.94(12)	2028.8(8)	1436.21(13)	5029.2(5)	2446.0(3)
Z	2	4	2	4	2
D_{calc} (g cm^{-3})	1.758	1.877	1.616	1.837	1.792
Number of unique reflections	7338	4124	8075	14667	14013
Number of observed reflections [$I > 2\sigma(I)$]	6780	3810	7707	10547	10575
R [$I > 2\sigma(I)$]	0.024	0.039	0.017	0.039	0.045
a, b for weighting scheme	0.029, 0	0.045, 15.279	0.019, 0.262	0.040, 0	0.041, 5.092
wR (all data)	0.059	0.097	0.041	0.085	0.109

solid after several minutes. The suspension was stirred at room temperature for 24 h, water (20 mL) added, and the white solid filtered off, washed with water (10 mL) and diethyl ether (10 mL) and dried under vacuum to give **13** (165 mg, 70%). M.p. 185–188 °C. *Anal.* Calc. for $C_{32}H_{32}N_6Au_2P_2S_2$: C, 37.7; H, 3.2; N, 8.2. Found: C, 38.2; H, 2.9; N, 8.2%. $^{31}P-\{^1H\}$ NMR, δ 37.3 (s). ^1H NMR, δ 7.83–7.23 (m, Ph), 6.0 (s, br, NH), 2.99 (m, Me). IR ν_{max} 2151 (s) and 1539 (s) cm^{-1}.

3.5. Crystallography

Intensity data for **1** and **10**–**12** were measured at 223 K (168 K for **8**) on a Bruker SMART CCD (Siemens SMART CCD for **8**) employing Mo Kα radiation so that $\theta_{max} = 30.0°$ (26.4° for **8**). The structures were solved by heavy-atom methods [33] (SHELXS-97 [34] for **8**) and refinement (anisotropic displacement parameters, hydrogen atoms in the riding model approximation and a weighting scheme of the form $w = 1/[\sigma^2(F_o^2) + (aP)^2 + bP]$ for $P = (F_o^2 + 2F_c^2)/3$) was on F^2 [35]. Complex **12** was characterised as its 1:1 CH_2Cl_2 solvate. Data manipulation was with teXsan [36] and crystallographic diagrams were drawn using ORTEP-II [37]. Crystallographic data and final refinement details are given in Table 3.

3.6. Biological assays

Assays were carried out by the commercial service offered by the Marine Chemistry Group, Department of Chemistry, Canterbury University, New Zealand. Samples were dissolved in 3:1 methanol–dichloromethane prior to testing. Cytotoxicity assays were carried out by determining, by means of a twofold dilution series, the concentration of sample in ng mL^{-1} required to reduce the cell growth of the P388 leukemia cell line (ATCC CCL 46) by 50%. The sample of interest was incubated for 72 h with the P388 Murine Leukemia cells. IC_{50} values were determined by measurement of the absorbance values when the yellow dye MTT tetrazolium is reduced by healthy cells to the purple dye MTT formazan.

The antimicrobial assays were carried out by measuring the inhibition zone as an excess radius (mm) from a 6 mm diameter filter paper disk containing 2 μg of sample, which was placed on a seeded agar plate containing the organism tested.

4. Supplementary material

Crystallographic data (excluding structure factors) for the structures described in this paper have been deposited with the Cambridge Crystallographic Data Centre, CCDC Nos. 273865–273869. Copies of the data can be obtained free of charge on application to The Director, CCDC, 12 Union Road, Cambridge CB2 1EZ, UK (fax: +44 1223 336 033; deposit@ccdc.cam.ac.uk or www: http://www.ccdc.cam.ac.uk).

Acknowledgements

We thank the University of Waikato and the National University of Singapore (NUS) for support of this work. We also thank Dr. Ralph Thomson for recording the NMR spectra, and Sarah Devoy for technical assistance. Professor Ward Robinson and Jan Wikaira (University of Canterbury, New Zealand) are thanked for collection of the X-ray data set of **8**. The State Government of Queensland is thanked for the award of a Smart Returns Fellowship to E.R.T.T.

References

[1] E.R.T. Tiekink, Gold Bull. 36 (2003) 117.
[2] E.R.T. Tiekink, Crit. Rev. Oncol. Hematol. 42 (2002) 225.
[3] S.Y. Ho, E.R.T. Tiekink, in: M. Gielen, E.R.T. Tiekink (Eds.), Metallotherapeutic Drug and Metal-based Diagnostic Agents, Wiley, New York, 2005, p. 421 (Chapter 22).
[4] M. Viotte, B. Gautheron, I. Nifant'ev, L.G. Kuz'mina, Inorg. Chim. Acta 253 (1996) 71.
[5] J.-C. Shi, L.-J. Chen, X.-Y. Huang, D.-X. Wu, B.-S. Kang, J. Organomet. Chem. 535 (1997) 17.
[6] V.W.-W. Yam, Pure Appl. Chem. 73 (2001) 543.
[7] M. Nakamoto, W. Hiller, H. Schmidbaur, Chem. Ber. 126 (1993) 605.
[8] S. Onaka, Y. Katsukawa, M. Shiotsuka, O. Kanegawa, M. Yamashita, Inorg. Chim. Acta 312 (2001) 100.
[9] B.-C. Tzeng, A. Schier, H. Schmidbaur, Inorg. Chem. 38 (1999) 3978.
[10] R. Narayanaswamy, M.A. Young, E. Parkhurst, M. Ouellette, M.E. Kerr, D.M. Ho, R.C. Eler, A.E. Bruce, M.R.M. Bruce, Inorg. Chem. 32 (1993) 2506.
[11] S.S. Tang, C.-P. Chang, I.J.B. Lin, L.-S. Liou, J.-C. Wang, Inorg. Chem. 36 (1997) 2294.
[12] W. Henderson, B.K. Nicholson, C.E.F. Rickard, Inorg. Chim. Acta 320 (2001) 101.
[13] W. Henderson, B.K. Nicholson, M.B. Dinger, R.L. Bennett, Inorg. Chim. Acta 338 (2002) 210.
[14] Y.-A. Lee, R. Eisenberg, J. Am. Chem. Soc. 125 (2003) 7778.
[15] M.W. Whitehouse, P.D. Cookson, G. Siasos, E.R.T. Tiekink, Metal-Based Drugs 5 (1998) 245.
[16] L. Hao, R.J. Lachicotte, H.J. Gysling, R. Eisenberg, Inorg. Chem. 38 (1999) 4616.
[17] P.D. Cookson, E.R.T. Tiekink, J. Chem. Soc., Dalton Trans. (1993) 259.
[18] M.C. Gimeno, E. Jambrina, E.J. Fernández, A. Laguna, M. Laguna, P.G. Jones, F.L. Merchán, R. Terroba, Inorg. Chim. Acta 258 (1997) 71.
[19] J.D.E.T. Wilton-Ely, A. Schier, N.W. Mitzel, S. Nogai, H. Schmidbaur, J. Organomet. Chem. 634–644 (2002) 313.
[20] B.F. Hoskins, Z. Lu, E.R.T. Tiekink, Inorg. Chim. Acta 158 (1989) 7.
[21] V.J. Hall, G. Siasios, E.R.T. Tiekink, Aust. J. Chem. 46 (1993) 561.
[22] H. Schmidbaur, Chem. Soc. Rev. (1995) 391.
[23] J.M. López-de-Luzuriaga, A. Sladek, W. Schneider, H. Schmidbaur, Chem. Ber. 130 (1997) 641.
[24] A. Sladek, K. Angermaier, H. Schmidbaur, Chem. Commun. (1996) 1959.
[25] A. Sladek, W. Schneider, K. Angermaier, A. Bauer, H. Schmidbaur, Z. Naturforsch. B 51 (1996) 765.
[26] A. Sladek, H. Schmidbaur, Chem. Ber. 128 (1995) 907.
[27] S. Wang, J.P. Fackler Jr., Inorg. Chem. 29 (1990) 4404.
[28] M.C. Gimeno, P.G. Jones, A. Laguna, M. Laguna, R. Terroba, Inorg. Chem. 33 (1994) 3932.
[29] C.A. McAuliffe, R.V. Parish, P.D. Randall, J. Chem. Soc., Dalton Trans. (1979) 1730.
[30] A.K. Al-Sa'ady, C.A. McAuliffe, R.V. Parish, J.A. Sandbank, Inorg. Synth. 23 (1985) 191.
[31] L.-T. Phang, T.S.A. Hor, Z.-Y. Zhou, T.C.W. Mak, J. Organomet. Chem. 469 (1994) 253.
[32] C.K. Mirabelli, D.T. Hill, L.F. Faucette, F.L. McCabe, G.R. Girard, D.B. Bryan, B.M. Sutton, J.O. Bartus, S.T. Crooke, R.K. Johnson, J. Med. Chem. 30 (1987) 2181.
[33] P.T. Beurskens, G. Admiraal, G. Beurskens, W.P. Bosman, S. García-Granda, J.M.M. Smits, C. Smykalla, The DIRDIF Program System, Technical Report of the Crystallography Laboratory, University of Nijmegen, 1992.
[34] G.M. Sheldrick, SHELXS-97: Program for the Solution of Crystal Structures, University of Göttingen, Göttingen, Germany, 1997.
[35] G.M. Sheldrick, SHELXL97: Program for the Refinement of Crystal Structures, University of Göttingen, Göttingen, Germany, 1997.
[36] teXsan: Structure Analysis Package, Molecular Structure Corporation, Houston, TX, 1992.
[37] C.K. Johnson, ORTEP-II, Report ORNL-5136, Oak Ridge National Laboratory, Oak Ridge, TN, 1976.